



# Laser cleaning and texturizing on high-speed steel tools for enhanced PVD process

M.S.F. Lima<sup>1</sup>, N.D. Vieira Jr.<sup>2</sup> & S.P. Morato<sup>3</sup>

<sup>1</sup> *Institute for Advanced Studies, Aerospace Technological Center, Brazil*

<sup>2</sup> *Center for Laser and Applications, IPEN, Brazil*

<sup>3</sup> *LaserTools Technologies Ltd., Brazil*

## Abstract

This work discusses the use of high-power Nd:YAG lasers to clean and texturize M2 tool steel surfaces. It is shown that surface ablation of the oxide layer was possible when the laser fluency was above  $0.4 \text{ J/cm}^2$ . Above this threshold, the surface presented craters due to the spread of the liquid metal. The region near to the surface was partly transformed from martensite to metastable austenite. The prior carbides were dissolved in the liquid metal and the martensite was decomposed during heating as can be seen in X-ray diffraction analyses. Physical vapor deposited layers of TiN were then applied to the modified surface. The present results had shown an increased surface adhesion of these coating after laser treatment in respect to conventional deposition.

## 1 Introduction

AISI M2 steels are high-speed tool materials consisting of carbides, martensite and some residual austenite, and present high hardness and good thermal stability [1]. These properties can only be obtained by a convenient heat treatment of the as-cast alloy. In general, this type of steel is maintained at some high temperature, e.g.  $1200 \text{ }^\circ\text{C}$ , to stabilize and to homogenize the austenite. This austenite is then transformed to martensite during quenching, thus giving a high toughness material. Further treatment at intermediate temperatures, e.g.  $560 \text{ }^\circ\text{C}$ , relaxes some of transformation stresses and

## 340 Computational Methods in Materials Characterisation

transforms the retained austenite to ferrite [2]. Once realized at normal atmosphere, these steps usually lead to surface contamination and to massive oxidation that must be removed either mechanically, e.g. by using sandblast, or chemically.

Laser cleaning offers competitive advantages to sandblast and chemical treatments because of the easy automation, the effluent elimination and the possibility to treat three-dimensional pieces, like drills and saw tips. Laser cleaning involves the removal of undesirable layers using short-time high-energy light pulses. The process can be athermal for the substrate when the layer is an oxidized film which detaches due to the rapid expansion of the brittle oxide metal together with the explosion of entrapped gases near metal-oxide interface [3]. Another possibility is the vaporization of a sub-micrometric layer by ablation [4]. Ablation is the effect of a rapid transition from superheated liquid to a mixture of vapor and liquid droplets [5]. Part of the incident heat can effectively be absorbed into the bulk material leading to local temperature changes and to structural modifications. These modifications can be useful for the material performance, depending on the desired application. Some laser cleaning techniques have used more power than needed to clean the surface to produce some surface roughness throughout melting (texturizing), since a slightly rough surface can present superior adherence to coatings [6]. These coating are hard materials which were used to decrease wearing and increase lifetime of tools.

The present study aims to establish a processing window for the elimination of oxidized layers on M2 steel samples using pulsed YAG lasers, as well as to investigate the microstructure modifications due to laser interaction. The adherence of TiN layers on the surface modified structure are then examined.

## 2 Experimental

A 15-mm diameter cylindrical M2 steel bar was cut in pieces of 5-mm height. These samples were annealed at 1200 °C for 10 minutes and then quenched in a vacuum chamber. After they were tempered at 560 °C under an atmosphere composed of N<sub>2</sub> and H<sub>2</sub>, twice, 2 hours each time. The layer thickness has some few nanometers, as measured by scanning electron microscopy in a region where a part of the layer was detached. Under this oxide layer, the as-tempered microstructure consisted of carbides embedded in a matrix of martensite and ferrite. The final hardness of the samples was between 62 and 64 HRC (Rockwell C test scale).

The laser was an active Q-switched Nd:YAG laser giving an energy per pulse in the range 0.1-8 mJ, a pulse length between 100 and 600 ns, and a pulse frequency in the range 1-50 kHz. The laser intensity at focus (0.8-mm diameter) was in the range  $4 \times 10^5$  -  $1 \times 10^7$  W/cm<sup>2</sup>.

Test surfaces of 3x3 mm<sup>2</sup> were scanned using a galvanometric head in line with the beam. The scanning was realized in a sequence of parallel lines at a fixed velocity and with 0.5 mm lateral shift. The laser experiments were

## Computational Methods in Materials Characterisation 341

repeated twice for each square with  $45^\circ$  tilt in order to uniform the energy distribution. The laser scanning velocity was 40 mm/s and all laser experiments were carried out in normal atmosphere.

Physical vapor deposition (PVD) of titanium nitride (TiN) was executed in a vacuum furnace. A coating of 2  $\mu\text{m}$  height was homogeneously applied to the extension of the laser-treated region. The sample temperature was kept below 500  $^\circ\text{C}$ .

Microstructural observations were carried out using optical and scanning electron microscopy. Optical microscopy employed standard polishing techniques and Nital 10% for chemical etching [1]. Scanning Electron Microscopy (SEM) analyses were carried out using secondary or back-scattered electron images. Secondary electrons image revealed the topography of the sample. Images from back-scattered electrons provided different contrasts for different phase densities. The identification of phases was achieved using X-ray diffraction (XRD) from the  $\text{CuK}\alpha$  radiation line.

A Rockwell C tester was used to induce surface cracks on the sample after TiN deposition in order to test the layer adhesion [7]. The inspection of cracking by scanning electron microscopy is good enough to establish the quality of layer-metal adherence.

### 3 Results

#### 3.1 Processing window

Different laser conditions were tested to check the efficiency of the oxide removal, as presented in Table 1. As it can be seen, a range of intensities from 0.4 to 9.8  $\text{MW}/\text{cm}^2$  was covered.

Table 1: Experimental parameters of laser processing

Exp.	$t_p$ (ns)	$E_p$ (mJ)	$\phi$ ( $\text{W}/\text{cm}^2$ )	f (kHz)
1	100	7.7	$9.8 \times 10^6$	1
2	100	6.2	$7.9 \times 10^6$	1
3	100	4.9	$6.2 \times 10^6$	1
4	100	3.2	$4.0 \times 10^6$	1
5	200	0.8	$9.8 \times 10^5$	10
6	200	0.6	$7.9 \times 10^5$	10
7	200	0.5	$6.2 \times 10^5$	10
8	200	0.3	$4.0 \times 10^5$	10

Legend:  $t_p$  is the pulse length,  $E_p$  is the energy per pulse,  $\phi$  is the intensity, f is the pulse frequency.

### 342 Computational Methods in Materials Characterisation

The experiments presented very good results for cleaning in all conditions except for the three lower power density tests (Table 1). The experiments 6 and 7 presented some residual oxide, particularly at the borders, and the Exp.8 did not affect the oxide layer. Figure 1 presents micrographs of different processing conditions.

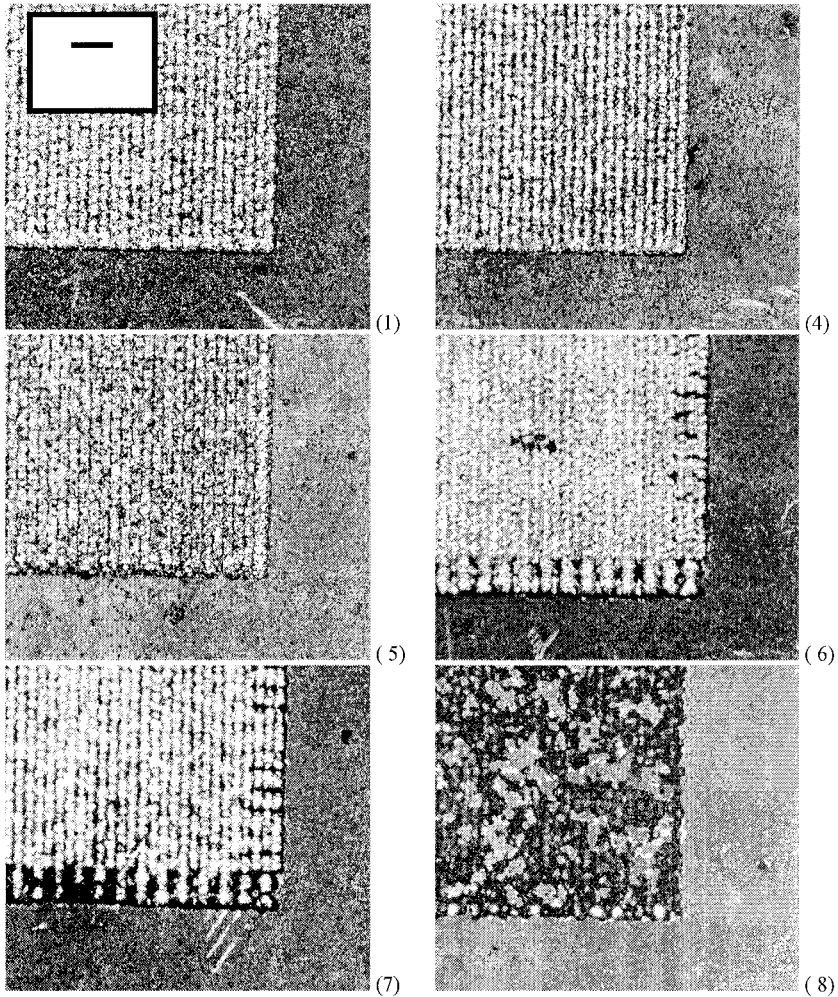


Figure 1: Effect of the laser parameters on the macrostructure of oxidized samples. Only borders are presented. The scale applies for all photographs. Numbers are referred in Table 1

### 3.2 Phase transformations

All successful experiments produced some surface melting of the metal. The surface was formed by a series of small liquid bath spots due to the pulsed laser. These laser marks produced only some small roughness for low power flux experiments and blow craters for the higher intensities, as shown in Figure 2.

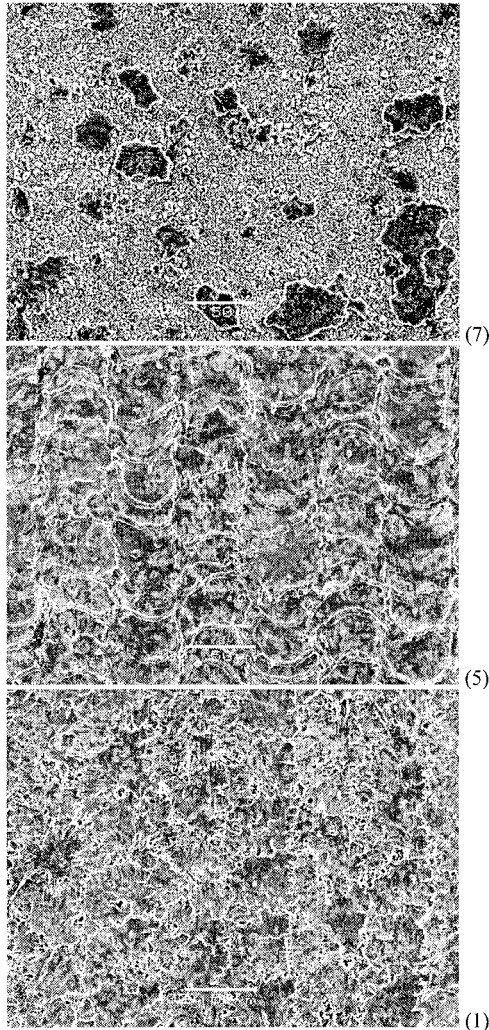


Figure 2: Scanning electron micrographs showing different surface qualities for different process parameters. Secondary electrons images (SEM). Numbers are referred in Table 1.

### 344 Computational Methods in Materials Characterisation

The melt depth was very thin in the experiments, as can be seen in the optical microscopy of a transversal section, Figure 3. The heat-affected zone was negligible and the maximum remelted depth is  $2\ \mu\text{m}$ , as presented in Figure 3 for the Exp.1.

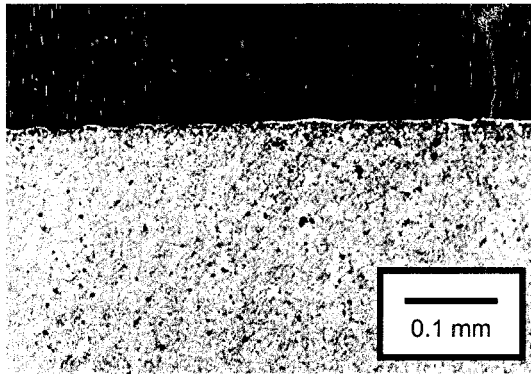


Figure 3: Optical micrograph of a transversal cut of the irradiated steel under AQS-3 condition. Laser processing was done in the upper surface. Optical microscopy. Etching: Nital 10%.

Figure 4 presents the XRD spectra of the M2 steel surfaces with the oxide layer, after being ground to the base material, and after the laser treatments. The diffraction peaks were assigned only once, although they were observed in the same angle for several spectra. The as-TT material consisted of martensite and  $\text{M}_6\text{C}$  carbides covered by an oxide layer (Ox) of  $\text{Fe}_2\text{O}_3$  and  $\text{Fe}_3\text{O}_4$ . The oxide peaks disappear from the spectra above AQS-9, showing the efficiency of the cleaning process over the Exp.5. Some carbide peaks can be also found in the experiments 5 and 7, because of uncompleted dissolution. The austenite ( $\gamma$ ) and martensite ( $\alpha$ ) phases were assigned with the respective Miller indexes. Austenite peaks were slightly distorted.

### 3.3 Surface adhesion

The experiment 5 was chosen to test the surface adhesion of a  $2\ \mu\text{m}$  TiN layer. Figure 5 shows the delamination marks of three different weights (60, 100 and 150 kg) on both polished and laser-treated surfaces. As can be seen, cracks were present in the polished sample up to the double of diameter of the diamond marks (150 kg). On the other hand, laser treated samples are crack free, showing increased adhesion between layer and steel.

## 4 Discussion

The mechanism of material removal is the laser ablation with vaporization of the base material. Using laser intensities on the range  $1\text{-}2 \times 10^8\ \text{W}/\text{cm}^2$  for

cleaning stainless steels after high temperature oxidation Psyllaki et alii concluded that the mechanism was mechanical [2]. For these authors the oxide is detached due to the stresses normal to the oxide/metal interface. The difference between the present and Psyllaki's results comes from the different pulse lengths, which were 10 ns for this author. It could be conceived that such short interaction time can produce a mechanical shock wave [8]. In the present case the process is clearly thermal; the ablation mechanism is more efficient and allows a larger processing window, even if it produces some metal losses.

The best results for ablation were obtained when using low-frequency high power pulses. The high peak power ablates efficiently the surface at same time that the relative low frequency avoids the local increase in temperature thus inhibiting re-oxidation. Although the process was carried out in normal atmosphere, the processed surfaces were brightly metallic.

One megawatt per square centimeter seems to be the minimum intensity allowing efficient surface cleaning. As can be seen in Figure 1, below this limit the borders were not very well defined and some oxides remained on the treated surface. Considering now the laser fluency instead of the intensity, one can correctly assign the lower limit for the laser of the surfaces as  $0.4 \text{ J/cm}^2$ . It is also suggested to employ a second processing step were the laser scanning is shifted  $45^\circ$  to regularize borders.

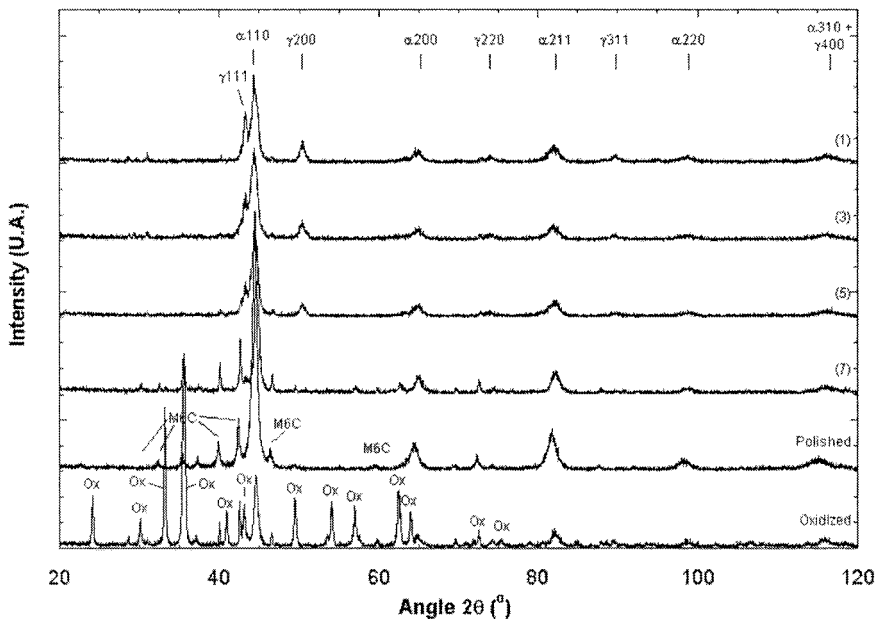


Figure 4: X-ray diffraction spectra of as-tempered and laser treated surfaces. See the text for legends.

## 346 Computational Methods in Materials Characterisation

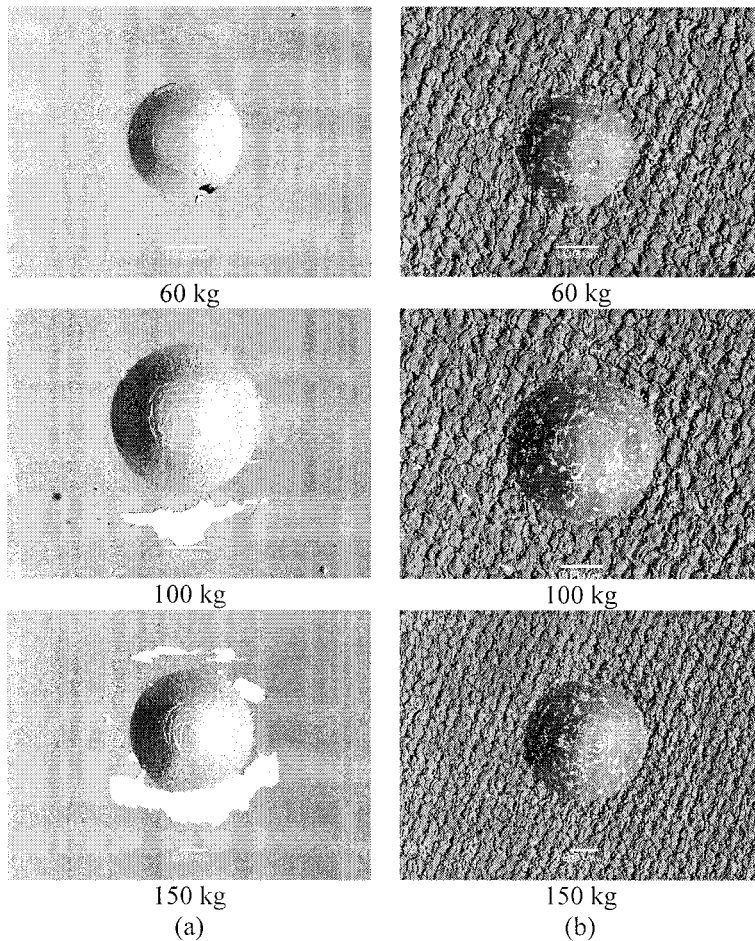


Figure 5: Scanning electron microscopy (Back-scattered electrons) of deposited TiN layers showing Rockwell C tests region. (a) Polished samples and (b) laser treated samples.

Laser surface treatment changes the microstructure and influences the macroscopic properties. During heating, the martensite is re-austenitized and the fine dispersion carbides were dissolved in the matrix. The result was some small composition variations at the surface which led to a variation in the lattice spacing of the austenite, as observed in the XRD spectra (Figure 4). Afterwards, since the cooling is rapid, the martensite was formed again but some residual austenite was preserved. The carbides cannot be formed under these conditions, leading to a surface layer with reduced hardness. However, this austenite has a high driving force for transformations, and it can be decomposed to ferrite plus carbides with a small increase in atomic mobility



due to heating. It could be realized that the superficial metastable layer can be also transformed during the tool use. The metastable austenite is then transformed to martensite due to mechanical stresses.

The surface properties after laser ablation present some interesting brand new features. First, the surface composition is more homogenous and thus the protective oxide layer can be formed. If this austenite-martensite layer must be reduced to a minimum, one could choose to use the lower effective cleaning intensity of the processing window, i.e. condition of Exp.5. Second, an enhanced adhesion to a deposited layer can be obtained as the roughness is changed through process parameter. In particular, it must be observed a low power intensity during processing because the blown craters in high-intensity tests forms metal tips (Figure 2), which will eventually detach near to the metal-coating interface.

The results of coating adhesion clearly show the advantages of the technique for key tooling applications (Figure 5). The enhanced adherence between layer and metal can be explained by the surface texturization which disrupt the shear stresses at the interface. As a result, deformation stresses are better distributed in the sample bulk and the coating remains as deposited.

## 5 Conclusions

The main conclusions of this work can be summarized in the following way:

- Complete surface cleaning of oxidized AISI M2 steel samples has been achieved. The best results were obtained using laser fluencies above  $0.4 \text{ J/cm}^2$  at processing speeds of 40 mm/s.
- The microstructure near the treated surface was changed. The martensite was decomposed in austenite and the carbides were dissolved in the matrix leading to a metastable structure.
- Texturization effects on the samples surface promoted high adherence of TiN layers on tool steel. This result is explained in terms of an improved distribution of stresses near the layer-metal interface.

## Acknowledgments

The authors would like to thank the Brazilian Synchrotron Light Laboratory (LNLS) for technical support. Thanks also are due to Professor Wilfried Kurz of the Department of Materials at the Swiss Federal Institute of Technology for the use of laboratory facilities. This work is funded by FAPESP-Fundação de Amparo à Pesquisa do Estado de São Paulo.



## 348 Computational Methods in Materials Characterisation

### References

- [1] American Society of Metals, Metals Handbook, vol 9, 9th edition, ASM, Metals Park, OH, USA, p. 256, 1985.
- [2] Speich, G.R., Leslie, W.C. , *Met. Trans.* **3A**, pp. 1043-1054, 1972.
- [3] Psyllaki, P. , Oltra, R. , *Mat. Sci Engineer.* **A282**, pp. 145-149. 2000.
- [4] Prokhorov, A. M. , Konov, V.I., Ursu, I., Mihailescu, I.N., *Laser Heating of Metals*, Adam Hilger Series on Optics and Optoelectronics, USA, pp. 108-113, 1990.
- [5] Kelly, R. , Miotello, A., *Appl. Surf. Sci.* **96-98**, pp. 205-210, 1996.
- [6] Coddet, C., Montavon, G., Ayrault-Costil, S., Freneaux, O., Rigolet, F., Barbezat, G., Folio, F., Diard, A., Wazen, P., *J. Thermal Spray Tech.* **8**, pp. 213-21, 1999.
- [7] Drory, M.D., Hutchinson, J.W. , *Proc. R. Soc. Lond A* **452**, pp. 2319-2321, 1996.
- [8] Jeong , S.H., Greif, R., Russo, R.E., *Applied Surf. Sci.* **127-129**, pp. 1029-1037, 1998.